

*From the Library of
Bret Leslie*

Level 4 Milestone for WBS 1.2.3.14.2

**Letter Report on Second Quarter Results of
Measurements in Hydrology Holes in the Single Heater
Test Area**

Deliverable ID: SP9216M4

Barry Freifeld & Yvonne Tsang

Earth Science Division
E. O. Lawrence Berkeley National Laboratory
1 Cyclotron Road
Berkeley, California, 94720

May 1997

Introduction

Measurements of changes in gas permeability during heating and cooling of the Single Heater Test (SHT) block can help to estimate the extent of moisture movement caused by the thermal load applied. Constant mass flux air injection tests, in addition to the continuous monitoring of relative humidity, temperature, and pressure, are being conducted in the SHT block in the two hydrology boreholes 16 and 18. The data obtained reveal the thermal-hydrologic response of the test block to heating, and give insight into the hydrologic response of the host rock to an emplaced waste package.

This report contains a preliminary analysis of the passive monitoring data collected from the start of testing, prior to heater turn on until March 7, 1997. These data consist of pressure, temperature, and relative humidity measurements made in zones isolated by pneumatic packers. In addition, the results of constant mass flux air injection tests performed in Boreholes 16 and 18 in the single heater test area on February 4-5, 1997 will be compared with the results of prior tests conducted on August 7-8, 1996, and November 25, 1996. A discussion of previous results for the first quarter air permeability measurements performed in the Single Heater Test Area can be found in Freifeld and Tsang, (1997).

Data Status and Quality Assurance

All field measurements were performed with qualified personnel and calibrated equipment under the LBNL QA program. All data presented are to be considered qualified data with the exception of measurements made by Humicap, serial number R2250005. Humicap R2250005 is located in ESF-TMA-NEU-2, commonly referred to as Single Heater Test Hole 16, and is used to monitor humidity and temperature in zones isolated by pneumatic packers. The Humicap failed to function normally after November 8, 1996, probably due to the submergence of the unit in condensate behind packer 16-4 (Figure 1). Since the Humicap sensor incorporates both the relative humidity measurement and the temperature, a post-test calibration on the Humicap sensor will be performed to determine the qualification of the temperature portion of the measurement, which continues to provide reasonable data.

One data file containing the results of injection testing is being submitted as part of this report. File FEBINJ.XLS includes data collected on February 4-5, 1996. The file is in Excel 7.0 PC format. Data from the malfunctioning Humicap sensor is not included. The data files are referenced with the data tracking number LB970500123142.001.

Testing Procedure

Boreholes 16 and 18 are instrumented with relative humidity, temperature, and pressure transducers. Each borehole contains four pneumatically inflated packers, labeled on Figure 1 as P₁, P₂, P₃, and P₄, designed to sustain the high temperatures expected during the SHT heating phase. Instrumented intervals are numbered from the closest to the collar of the borehole, 1, to the deepest zone, behind the last packer in the string, 4. The eight instrumented intervals are referred to by borehole number followed by the zone number, e.g., 18-3 is the third instrument cluster from the collar in Hole 18. The pressure, temperature, and relative humidity sensors are all located just below the packer (deeper in the borehole) and are assigned the same numeric identifier as the packer just above them.

Each interval between packers, and one interval past the end of the last packer, is fitted with a ¼ inch Teflon injection tube. Dry, clean compressed air is regulated using mass flow controllers and injected into the designated zone. By selectively deflating different packers, various injection zones for each hydrology hole are formed. Illustrated in Figure 1 are three possible test configurations: (1) deflate packer P₂ and use air injection line for P₁, (2) deflate packer P₃ and use air injection line for P₂, (3) inflate all four packers and use the air injection line for P₄. These three configurations are denoted as injection zones Zone 1, Zone 2, and Zone 3 respectively in Figure 1. All four packers in the monitoring hole are always inflated so that pressure response can be monitored in each of the four sensors.

While a test is conducted, the temperature and pressure are continuously monitored. Table 1 summarizes the instrumentation in Boreholes 16 and 18 and the location in the monitoring data file where the measurements can be found. During injection testing, data were collected at 5-second intervals early in the test period, and as the test approached steady state, the data logging interval was increased. Table 2 summarizes the tests that were conducted. When it is noted that a test was conducted between two packers (e.g. between 18-1 and 18-3), this indicates that the packer(s) in the interval between the listed packers was deflated during the test.

Analysis and Results

Permeability Measurements

When possible, injection tests were conducted until a steady state response occurred. The flow rate and change in pressure at steady state, under the assumption of isothermal conditions, was used to estimate the permeability for the test zone using the following formula:

$$k = \frac{P_{sc} Q_{sc} \mu \ln\left(\frac{L}{r_w}\right)}{\pi L (P_2^2 - P_1^2)}$$

where

k = permeability, m^2

P_{sc} = pressure at standard conditions, 1.013×10^5 Pa

Q_{sc} = flowrate at standard conditions, $m^3 s^{-1}$

μ = dynamic viscosity of air, 1.81×10^{-5} Pa-s (at 20°C)

L = length of air injection zone, m

r_w = radius of borehole, m

P_2 = steady state injection pressure, Pa

P_1 = ambient pressure, Pa

Calculated permeabilities are shown in Table 2 for each test conducted. Figure 2 shows the transient pressure response to the constant mass flux injections. A striking feature noted in these tests is the qualitative difference of pressure responses between injections in the Zone 3 locations and injections in Zone 1 and Zone 2. While injections in Zone 1 and 2 show the expected buildup in pressure, Zone 3 shows a pressure buildup followed by a gradual decrease. It is thought that this decrease is due to the transport of moisture, present as thin films on fracture surfaces and trapped in portions of fractures with small apertures, away from the test location by the dry injected gas, thereby increasing air permeability. This behavior was also observed during the ambient phase preheating injection tests (Tsang et. al., 1996).

Calculated permeabilities for the February 4-5 injection tests have been compared with the previous test results in Table 3. In Table 3, data in the first two rows correspond to the test configuration where the air injection is in Zone 3, data in the third row correspond to air injection in Zone 2, and data in the fourth and fifth rows correspond to air injection in Zone 1.

As discussed in detail in our First Quarter report (Freifeld and Tsang, 1997) we anticipated a reduction in air permeability from its pre-heating values in Zone 3 and not in Zones 1 and 2. This is attributed to the fact that Zone 3 resides in the condensation zone of the SHT. The air permeability remaining practically unchanged from the first quarter to the second quarter of heating can be understood as follows. We note from the

temperature monitoring data of the SHT that the volume of rock bound by the 100°C isotherm rises rapidly from 0 to 16.6 m³ in the first 96 days of heating (November 30, 1996), and increases much more slowly to 20.7 m³ on February 17 (day 175 after the start of heating). Therefore, most of the condensation buildup in Zone 3 occurs in the first three months of heating and accounts for the majority of the air permeability decrease derived from the first quarter air injection tests.

Pressure transient responses for earlier injection tests, conducted on August 7-8 and on November 25 are shown in Figure 3 and Figure 4. To emphasize the changes in permeability due to heating, air injection tests conducted in Borehole 16, Zone 3 are presented in Figure 5. Most noticeable in the post-heating pressure response curves is the absence of any significant intraborehole responses. Figure 6 shows that Zone 3 in Borehole 16 has a larger response due to air injection tests conducted in borehole 18 after heater turn on. These seemingly contradictory responses are interpreted as changes in the plumbing of the fracture network, due to the redistribution of moisture away from the heater.

Temperature Measurements

Temperature monitoring data through March 1997 (Homuth, 1996, 1997) are shown in Figure 7. Although the data are collected once per hour, only one point per day is plotted. Note that from November 10 through November 14, the temperature reading in Sensor 16-4 is spurious. The anomalous readings with the sensor occurred at the same time as when the Humicap 16-4 became non-functional, probably due to condensate in the zone. After this period, the temperature sensor seems to have recovered and gives reasonable readings, though fluctuations beyond the expected range still persist. Figure 7 shows the predictions from the 3D hydrological simulations of the SHT (Birkholzer and Tsang, 1996) indicated by open circles. It is clear that the simulated results slightly underpredict the first quarter temperature measurements, and overpredict by a larger degree the measurements at six months after heating.

The discrepancy between simulated results and measurements can possibly be attributed to the thermal conductivity parameter used in the modeling exercise. At the time of simulations (Birkholzer and Tsang, 1996), the site specific thermal conductivity measurements available to the modelers were those of air-dry rock cores from the SHT with a value of 1.67 W/mK (CRWMS M&O Report, 1996). Newer simulations, not presented here, use a thermal conductivity that is a function of matrix saturation. At present it has been determined (Nancy Brodsky, SNL, Personal communication, 1997) that the thermal conductivity of the saturated rock cores from the SHT is more on the order of 2 W/m²K. Recall that all the sensors 1 through 4 in both Holes 16 and 18 lie outside the dry-out zone of the SHT, and therefore will be better represented by a higher thermal conductivity than that used in the simulations. At the early time, the use of the erroneously low thermal conductivity means that the simulations will overpredict temperature near the heater and underpredict the temperatures outside of the boiling zone, which accounts for the prediction of November 1996. As the test proceeds and the

volume of heated rock mass expands, the use of the erroneously low thermal conductivity means that heat is not being carried away fast enough, which in turn means overprediction occurs at all sensors, more so in the sensor 4 which situates in the wettest region. Therefore, the discrepancy of the actual thermal conductivity deviates the most from that utilized for the simulations.

Relative Humidity Measurements

Relative humidity measurements for the first 6 months of heating are shown in Figure 8. These measurements have an accuracy of $\pm 2\%$ below 90% RH and an accuracy of $\pm 3\%$ RH above that point. The relative humidity sensor is effective in monitoring very dry rock mass with strong capillary suction, but is not sensitive to "normal" liquid saturation. That is, unless the rock mass is very dry, the relative humidity sensor is expected to register 100%. It is therefore our expectation that all the sensors in Holes 16 and 18 should register effectively 100 (± 3)% before turning on of the heat. Moreover, since even the sensors closest to the single heater are at least 3 meters from the heater and, based on the thermal-hydrological simulations (Birkholzer and Tsang, 1996), lie outside the drying zone throughout one year of heating, the readings of the Humicaps are expected to continue to register 100% during heating.

The monitoring data in Figure 8 display that by the first week of September, the vapor phase in the monitoring zones in Holes 16 and 18 have come into equilibrium with the liquid in the rock mass and the readings in Sensors 16-4 and 18-4 stabilize to 100%. However, the relative humidity measurements displayed in Figure 8 show that the three measurements closest to the collars are between 86% and 94% RH and remain somewhat constant in the six months of heating. Relative humidity can be related to moisture potential (given in Pascals) using the Kelvin equation,

$$\mu = \frac{\rho RT}{M} \ln(RH)$$

where

μ = moisture potential Pa

ρ = density of the fluid, gm m⁻³

R = the universal gas constant, 8.3145 Pa m³ mol⁻¹ K⁻¹

T = temperature, K

M = gm molar weight of the fluid, gm mol⁻¹

RH = relative humidity.

The moisture potential which corresponds to an RH value of 90% at 30°C is -14.7 MPa. This is not consistent with the matrix liquid saturation obtained for grab samples collected in the SHT area which is reported to be between 80 and 99% (Tsang et al., 1996). Matrix samples with saturations as high as 80% would have a corresponding RH very near 100%. One possible explanation of observed low values of relative humidity is drying due to the effects of tunnel excavation. Due to ventilation, the ESF has a relative humidity that fluctuates between 20% to 80% RH (Wang et al., 1996), and the boreholes appear to be in communication with the drift through the fractures in the rock mass. If moisture transport out of the matrix is the cause of the low formation RH readings, it should be noted that the depth at which this dryout region extends is greater than predicted by the numerical modeling studies presented in Wang et al., 1996.

Pressure Measurements and Flux of Condensate into Borehole 16, Zone #3

Gauge pressure monitoring data are presented in Figure 9. It is expected that no significant pressure buildup will occur due to heating, since the heater borehole is in direct communication with the thermal drift. All pressure transients, except for those recorded in 16-4, show no significant pressure variation from the ambient.

The pressure response in 16-4 has been replotted in Figure 10. The buildup in pressure corresponds to the buildup of condensate in Zone 3 of Borehole 16. Each drop in pressure corresponds to the three times that water was drained from Zone 3, on November 25, 1996; February 4, 1996; and February 27, 1997.

Based upon the volume of the sample collected and the time elapsed between samplings, the rate at which condensate is infiltrating into Zone 3 can be calculated. Using the change in the pressure head measured immediately before and after sampling along with the geometry of the borehole, we can perform a check on the infiltration rate calculated. This verifies that the pressure buildup is due to condensate collection in Zone 3. A correction on the infiltration rate for the first sampling has to be performed, since the tube from which the sample is drained is spatially higher than the pressure transducer. A residual amount of water will remain in Zone 3 after draining, which creates the offset of .9 kPa of the post sampling pressure from the pressure recorded before heating was started. Table 4 shows the results of the above calculations.

It is interesting to note that within one week of August 26, the heater turn-on date, condensate began to increase the pressure in Zone 3. It is also apparent that the rate at which condensate is entering the borehole has tapered off from the initial rate observed during October and November of 1996. This reduction in condensate flux is quantified in Table 4 and is visible in the pressure measurements shown in Figure 10.

Summary

Cross hole air injection tests as well as passive monitoring of temperature, relative humidity, and pressure are continuing to be conducted in the Single Heater Test area. Many of the observed responses to heating are understood and predictable, such as the

rate at which heat is transported through the formation. Observations such as the dryout zone in the formation adjacent to the ventilated tunnel and the flow of condensate into Zone 3 of Borehole 16 require closer examination of the responsible processes. The knowledge that is gained through the analysis of the SHT data provides insight into expected behavior due to thermal loading imposed by emplaced radioactive waste canisters. The SHT data provides field scale baseline estimates of transport parameters, which can subsequently be used for predictive modeling of the Drift Scale Test experiment.

Acknowledgment

The authors wish to thank Jens Birkholzer and Kenzi Karasaki for their review and comments. This work was supported by the Director, Office of Civilian Radioactive Waste Management, U.S. Department of Energy, through memorandum Purchase Order EA9013MC5X between TRW Environmental Safety Systems, Inc. and the Ernest Orlando Lawrence Berkeley National Laboratory, under contract No. DE-AC03-76SF00098.

References

Birkholzer, J. and Y. Tsang, 1996, Forecast of thermal-hydrological conditions and air injection test results of the Single Heater Test, Level 4 milestone SP918M4, LBNL, Berkeley, CA.

CRWMS M&O Report B00000000-01717-5705-00047, 1996, Characterization of the ESF Thermal Test Area, 1996.

Freifeld, B., and Y. Tsang., 1997, Letter report on first quarter results of measurements in hydrology holes in Single Heater Test area in the ESF, Level 4 Milestone for WBS 1.2.3.14.2, DTN: LB970100123142.001, LBNL, Berkeley, CA.

Homuth, Fred, 1996, 1997, Monthly memos to Single Heater Test Principal Investigators regarding transfer of data from ESF Data Collection Systems, Memorandum LA-EES-13-LV-11-96-041, LA-EES-13-LV-12-96-008, LA-EES-13-LV-01-97-019, LA-EES-13-LV-02-97-019, LA-EES-13-LV-03-97-004, LA-EES-13-LV-04-97-002.

Tsang, Y., J. Wang, B. Freifeld, P. Cook, R. Suarez-Rivera, T. Tokunaga, 1996, Letter report on hydrological characterization of the Single Heater Test area in the ESF, Level 4 Milestone for WBS 1.2.3.14.2, August 1996, DTN: LB960500834244.001, LBNL, Berkeley, CA

Wang, J., A. Flint, J. Nitao, D. Chesnut, P. Cook, N. Cook, J. Birkholzer, B. Freifeld, L. Flint, K. Ellet, A. Mitchell, F. Homuth, G. Griego, J. Cerny, and C. Johnson, 1996, Evaluation of moisture evolution in the Exploratory Studies Facility, Yucca Mountain Project Level 4 Milestone TR31K6M, DTN: LB960800831224.001, LBNL, Berkeley, CA

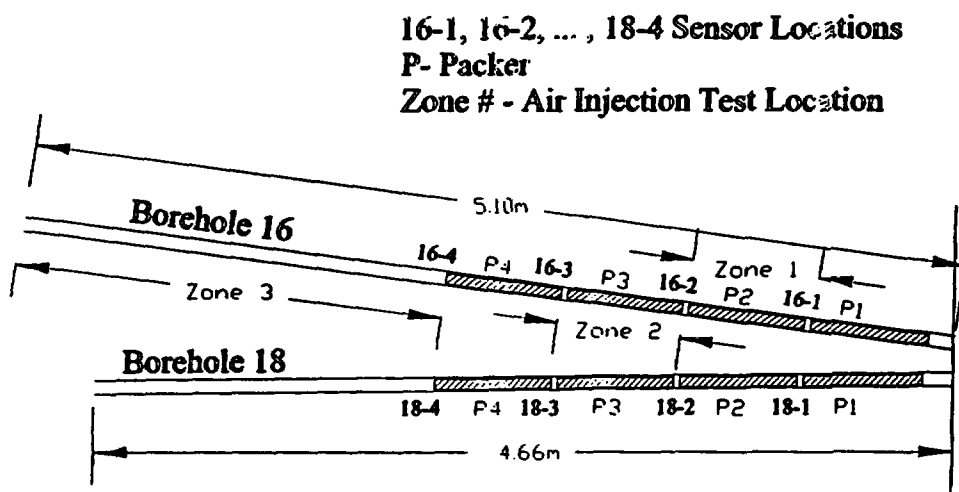
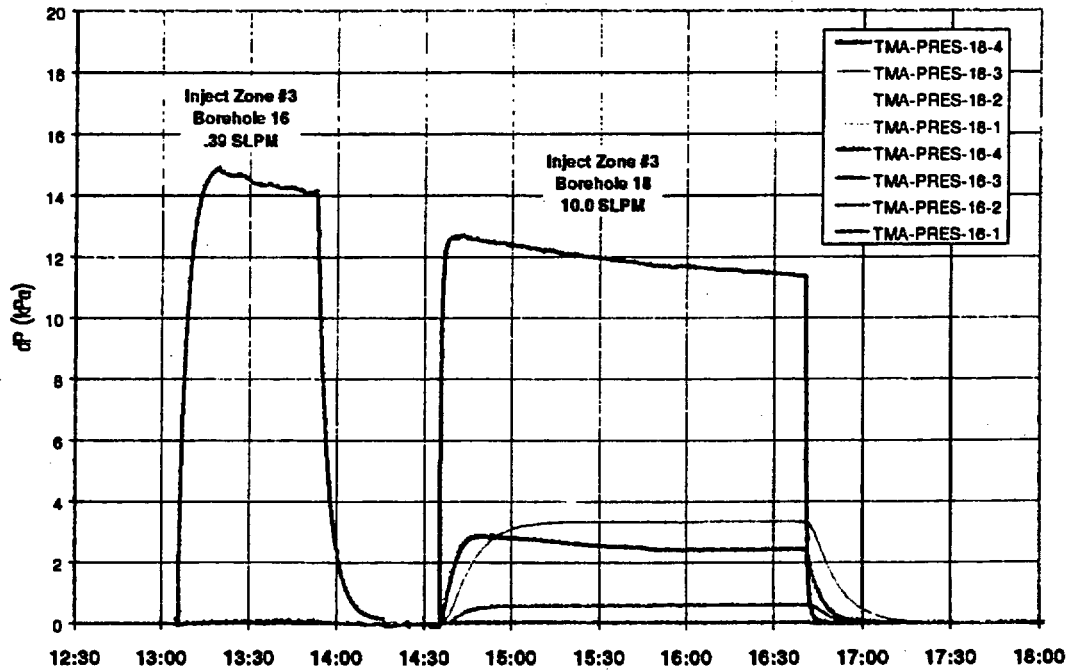


Figure 1. Geometry of the air injection test boreholes and instrumentation. Injection zone 1 is created by deflating P2 and zone 2 is created by deflating P3.

SHT 2/4/97 Air Injection



SHT 2/5/97 Air Injection

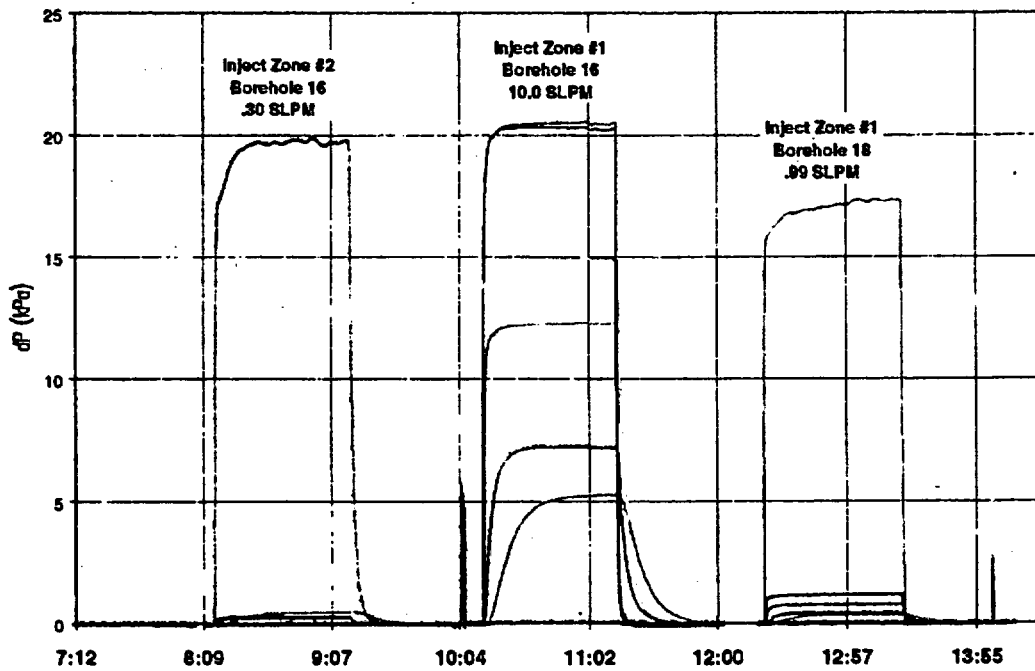


Figure 2. Pressure transients for air injection tests conducted on February 4 and 5, 1997.

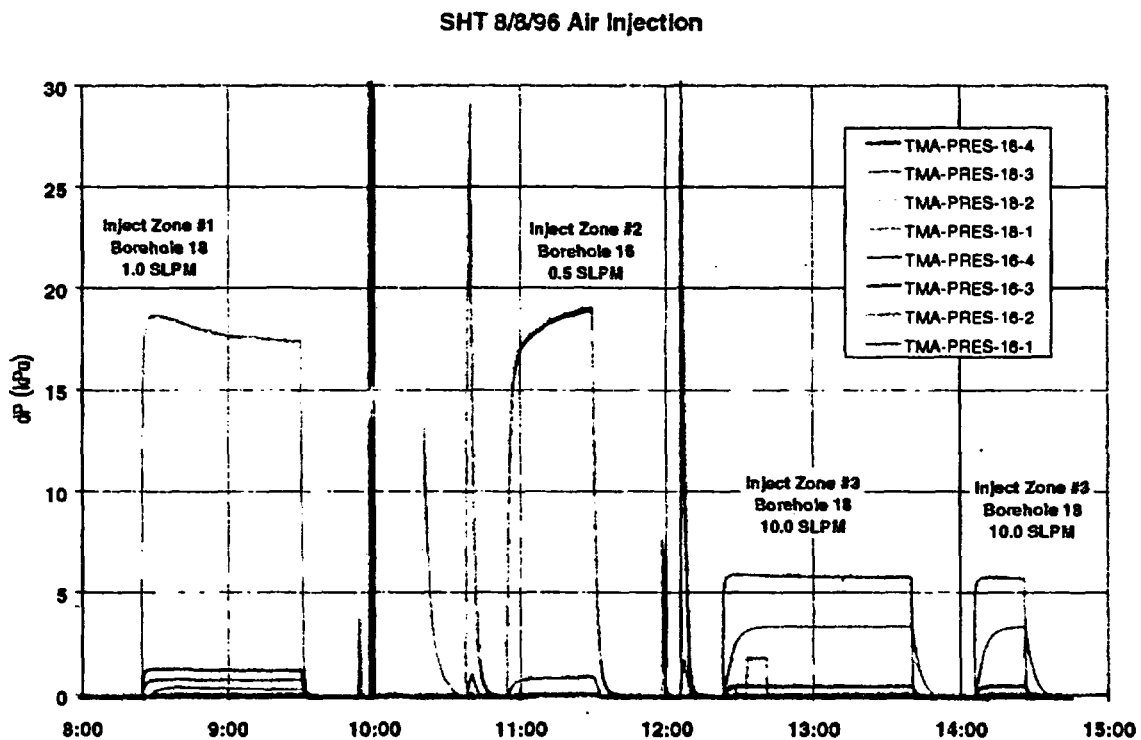
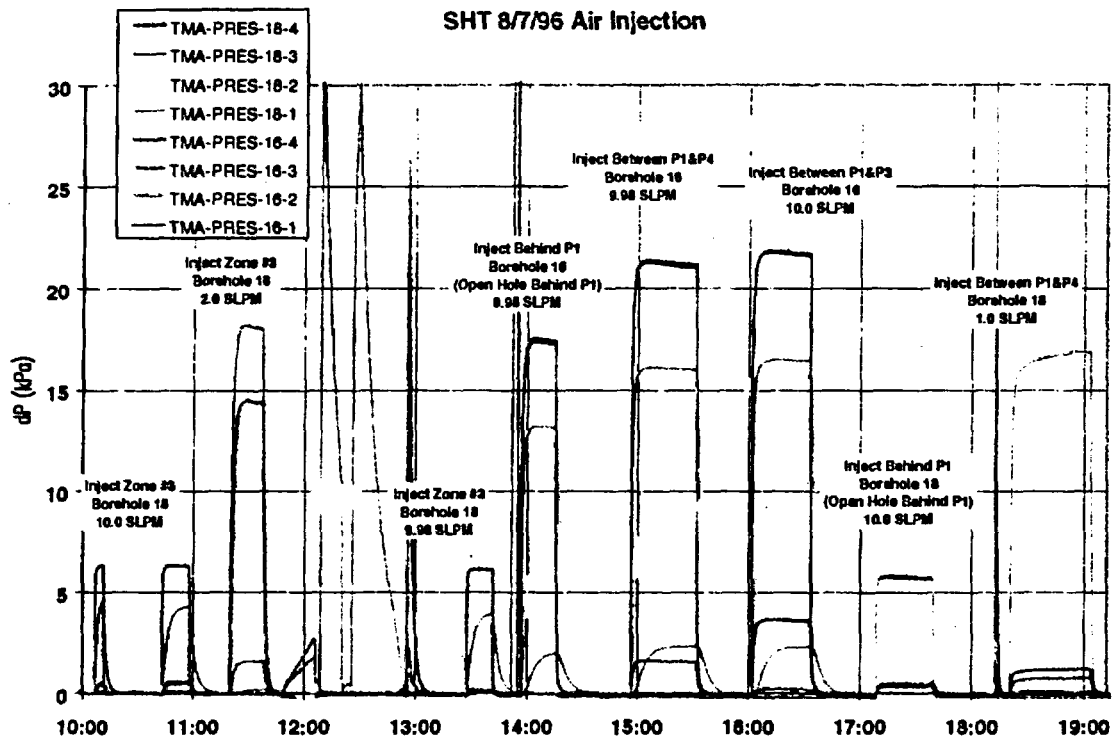


Figure 3. Pressure transient for pre-heating air injection tests conducted on August 7 and 8, 1996. Due to low permeabilities in a few tests sections, some tests were aborted when a rapid rise in zone pressure was noticed.

SHT 11/25/97 Air Injection

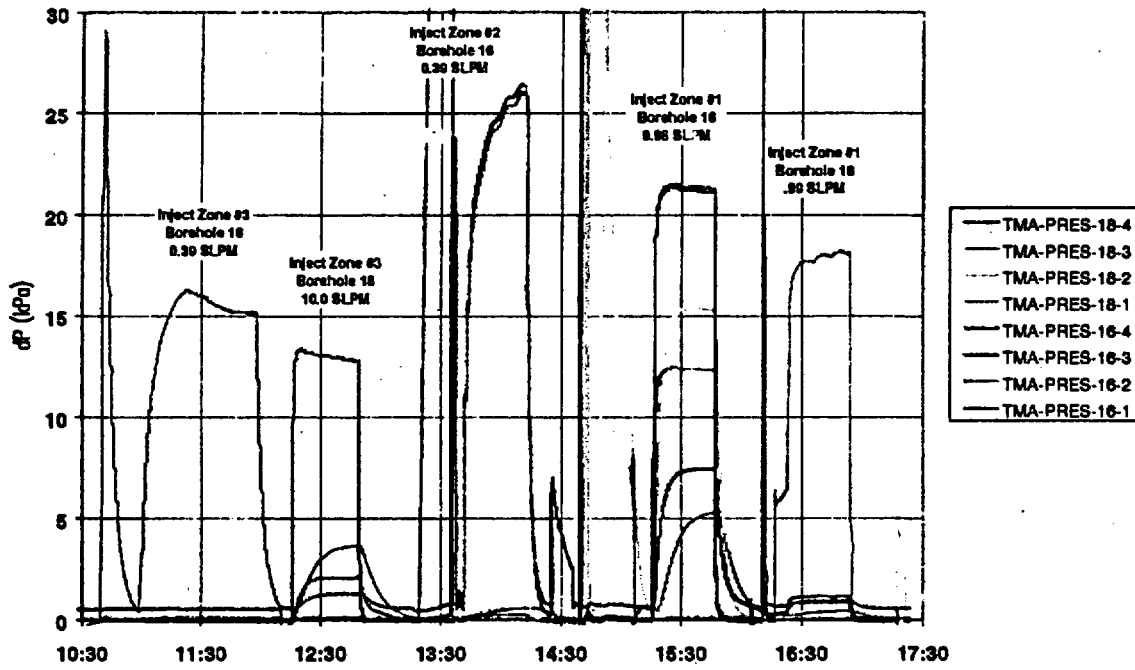
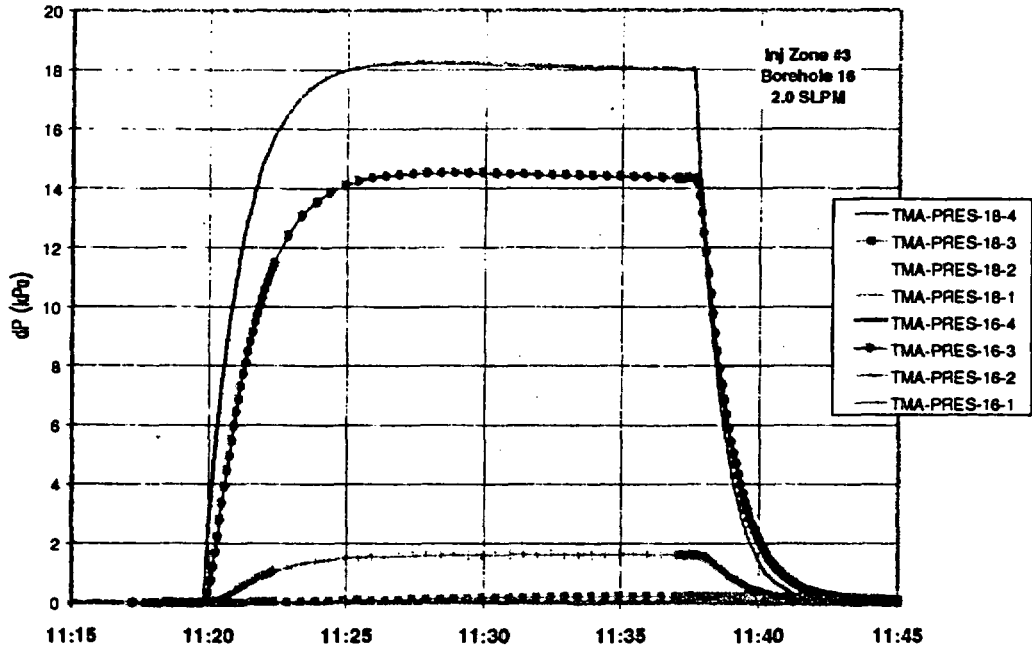


Figure 4. Pressure transients for air injection tests conducted on November 25, 1996.

SHT 8/7/96 Air Injection



SHT 2/4/97 Air Injection

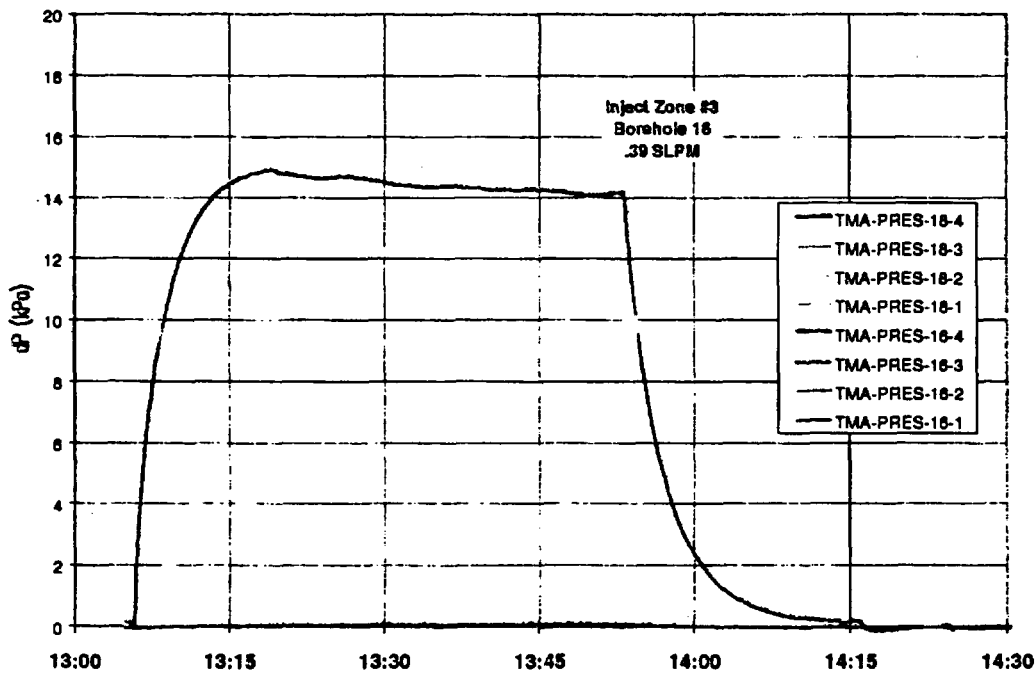
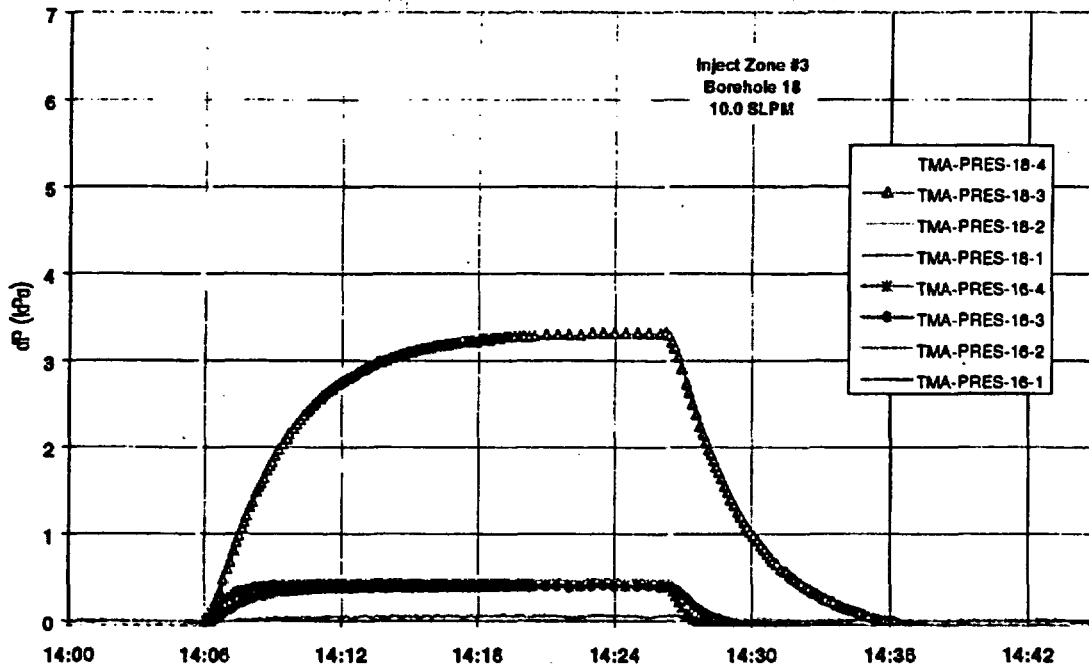


Figure 5. Comparison between air injection tests conducted before heating and after heating shows a significant drop in cross zone permeability. Measurements made on 2/4/97 were conducted after water was drained from borehole 16, Zone 3.

SHT 8/8/96 Air Injection



SHT 2/4/97 Air Injection

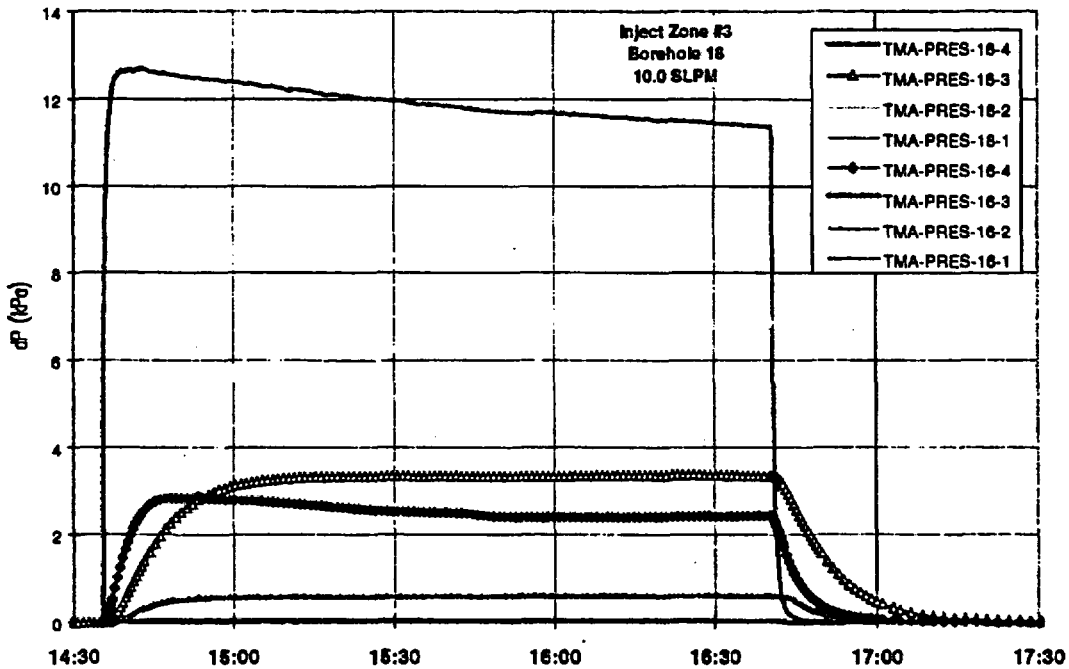


Figure 6. After heating, the magnitude of the crosshole response in borehole 16, Zone 3 due to injection in borehole 18, Zone 3 is seen to increase.

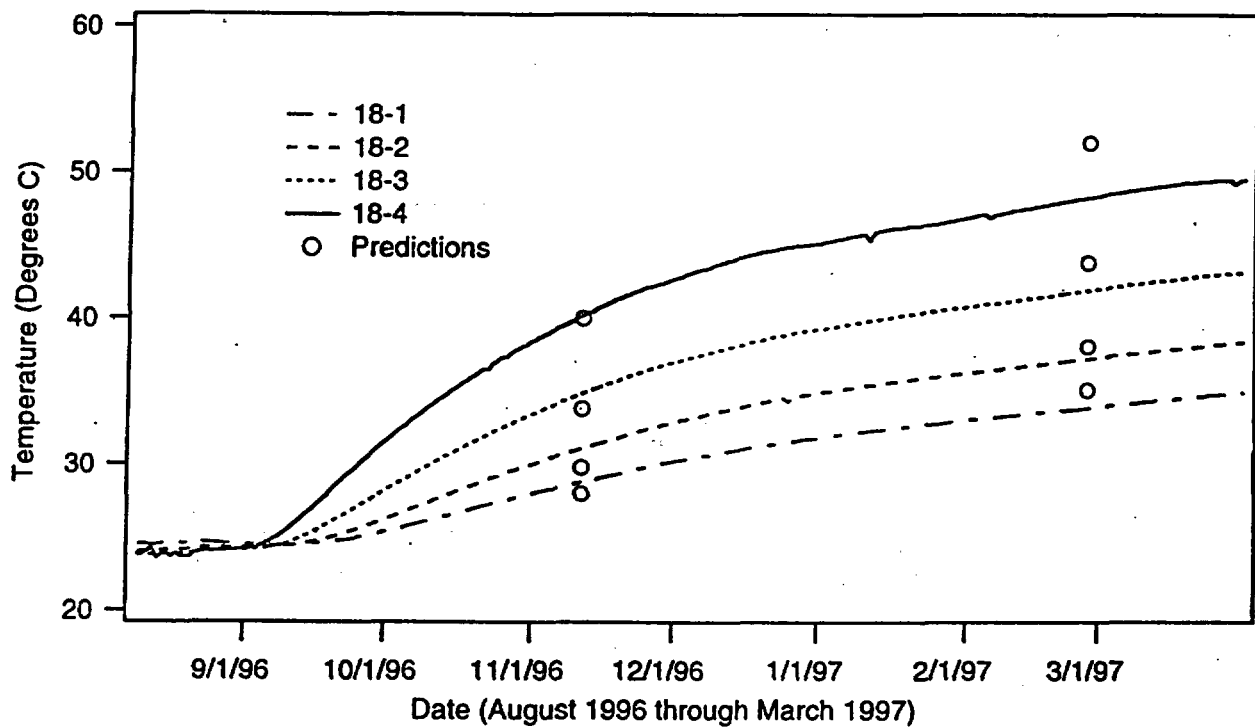
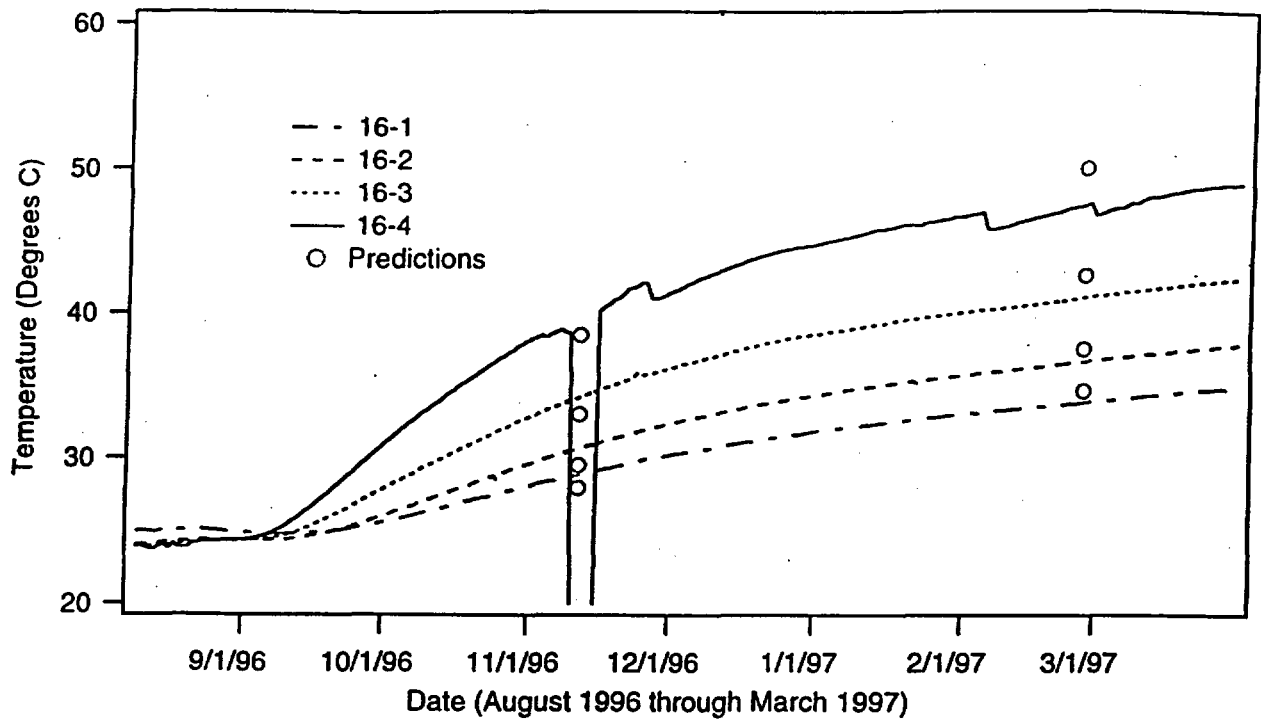


Figure 7. Temperature data measurements made in boreholes 16 and 18 compared with model predictions.

SHT Relative Humidity Measurements

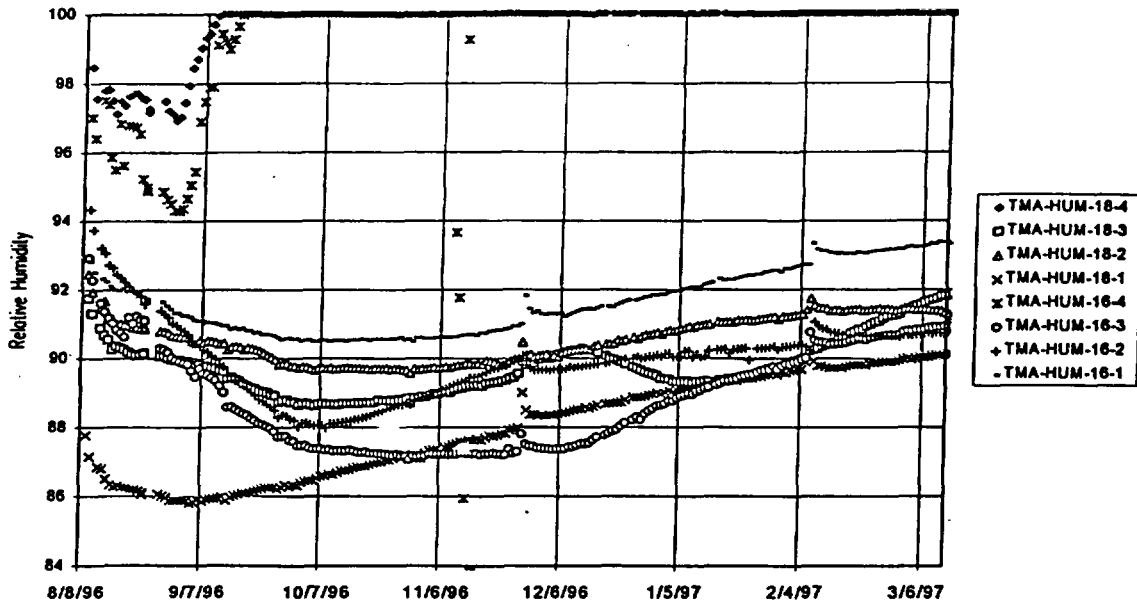


Figure 8. Relative humidity measurements made away from the heated drift show a surprisingly low value indicating significant drying of the rock closest to the drift may have occurred. Small perturbations occur due to air injection tests.

SHT Pressure in Boreholes #16 & #18

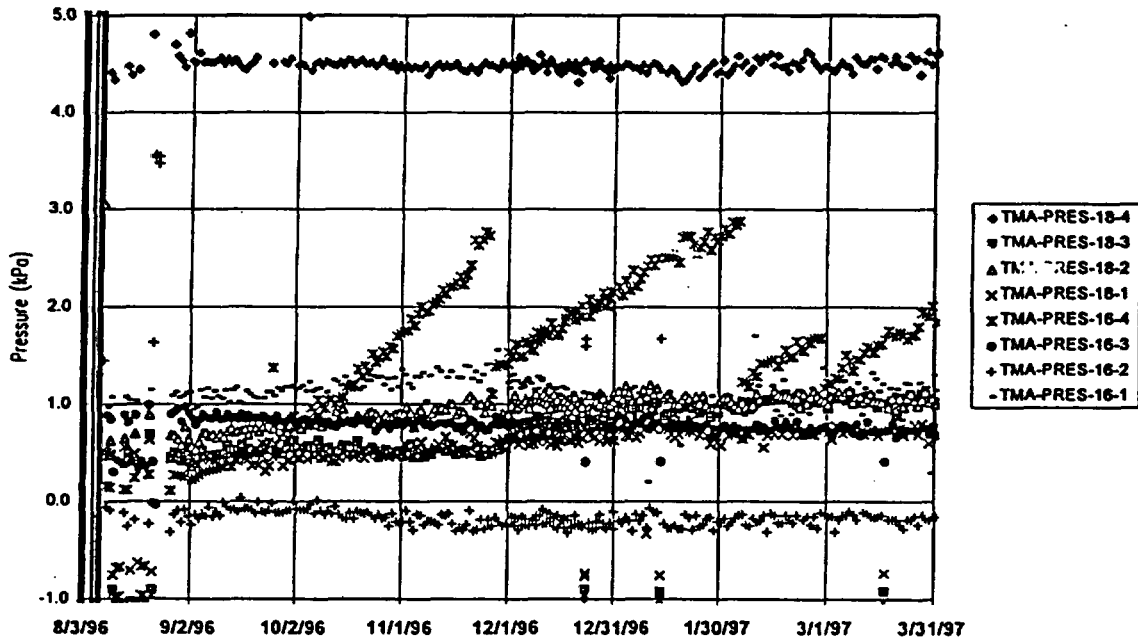


Figure 9. Gauge pressure measurements recorded by transducers mounted within the isolated intervals. Starting pressure offsets from 0 are due to sensor zero shift.

TMA-PRES-16-4

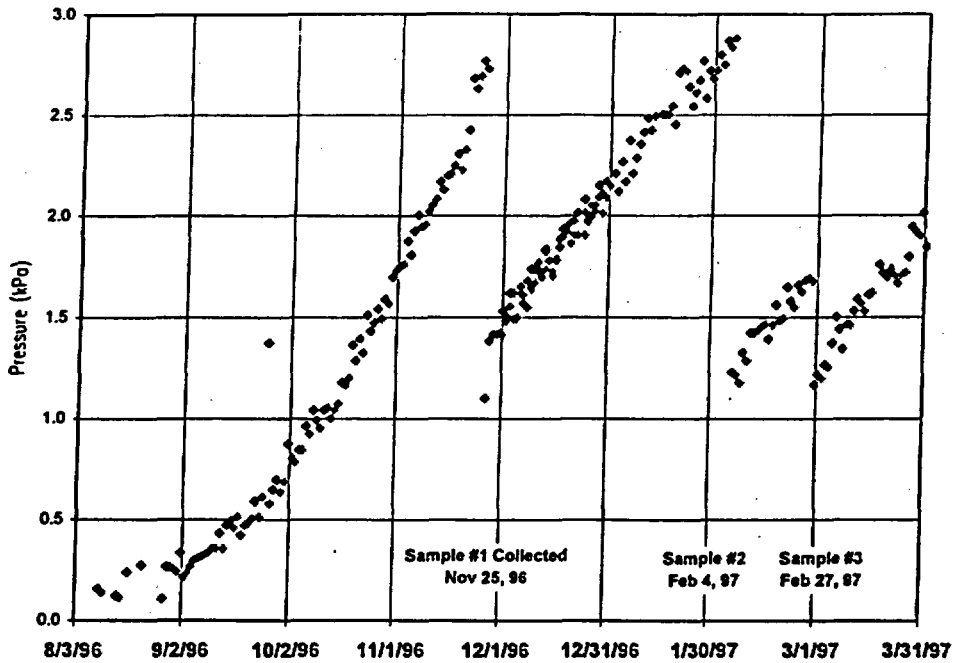


Figure 10. Gauge pressure measurements in Borehole 16, Zone 3 increases due to the buildup of condensate in the zone. Drops in pressure are due to the periodic collection of water samples.

Table 1. Instrumentation in the SHT block hydrology holes #16 and #18.

Column	Sensor Location	Parameter Measured	Units	Alcove Sensor Name
1	N/A	Date/Time	N/A	N/A
2	Hole #18 Zone 4	Δ Pressure	kPa	TMA-PRES-18-4
3	Hole # 18 Zone 3	Δ Pressure	kPa	TMA-PRES-18-3
4	Hole # 18 Zone 2	Δ Pressure	kPa	TMA-PRES-18-2
5	Hole # 18 Zone 1	Δ Pressure	kPa	TMA-PRES-18-1
6	Hole #16 Zone 4	Δ Pressure	kPa	TMA-PRES-16-4
7	Hole #16 Zone 3	Δ Pressure	kPa	TMA-PRES-16-3
8	Hole #16 Zone 2	Δ Pressure	kPa	TMA-PRES-16-2
9	Hole #16 Zone 1	Δ Pressure	kPa	TMA-PRES-16-1
10	Hole # 18 Zone 4	Relative Humidity	%	TMA-HUM-18-4
11	Hole # 18 Zone 4	Temperature	$^{\circ}$ C	TMA-TEMP-18-4
12	Hole # 18 Zone 3	Relative Humidity	%	TMA-HUM-18-3
13	Hole # 18 Zone 3	Temperature	$^{\circ}$ C	TMA-TEMP-18-3
14	Hole # 18 Zone 2	Relative Humidity	%	TMA-HUM-18-2
15	Hole # 18 Zone 2	Temperature	$^{\circ}$ C	TMA-TEMP-18-2
16	Hole # 18 Zone 1	Relative Humidity	%	TMA-HUM-18-1
17	Hole # 18 Zone 1	Temperature	$^{\circ}$ C	TMA-TEMP-18-1
18				
19				
20	Hole #16 Zone 3	Relative Humidity	%	TMA-HUM-16-3
21	Hole #16 Zone 3	Temperature	$^{\circ}$ C	TMA-TEMP-16-3
22	Hole #16 Zone 2	Relative Humidity	%	TMA-HUM-16-2
23	Hole #16 Zone 2	Temperature	$^{\circ}$ C	TMA-TEMP-16-2
24	Hole #16 Zone 1	Relative Humidity	%	TMA-HUM-16-1
25	Hole #16 Zone 1	Temperature	$^{\circ}$ C	TMA-TEMP-16-1
26	N/A	Endevco Input Voltage	Volts	N/A

Table 2. Injection tests conducted in the SHT block.

Date	Test Description (In the order they were conducted)	Q(SLP M)	dP (Pa)	Length (m)	Permeability (m ²)
4-Feb-97	Inj Behind 16-4	0.39	14730	2	2.67E-15
4-Feb-97	Inj Behind 18-4	10.0	12650	2	8.05E-14
5-Feb-97	Inj Between 16-2, 16-4	0.30	19930	0.762	3.81E-15
5-Feb-97	Inj Between 16-1, 16-3	9.98	20290	0.762	9.56E-14
5-Feb-97	Inj Between 18-1, 18-3	0.99	17430	0.762	1.12E-14
25-Nov-96	Inj Behind 16-4	0.39	15190	2	2.58E-15
25-Nov-96	Inj Behind 18-4	9.96	12770	2	7.93E-14
25-Nov-96	Inj Between 16-2,16-4	0.39	26000	0.762	2.83E-15
25-Nov-96	Inj Between 16-1,16-3	9.95	21300	0.762	9.03E-14
25-Nov-96	Inj Between 18-1,18-3	0.99	18000	0.762	1.08E-14
7-Aug-96	Inj Behind 18-4	2	1100	2	1.97E-13
7-Aug-96	Inj Behind 18-4	10	6300	2	1.67E-13
7-Aug-96	Inj Behind 16-4	2	18000	2	1.10E-14
7-Aug-96	Inj Behind 18-4	9.98	6100	2	1.73E-13
7-Aug-96	Inj Behind 16-1 (Open hole behind)	9.98	17400	4.1	3.28E-14
7-Aug-96	Inj Between 16-1, 16-4	9.98	21300	1.46	5.75E-14
7-Aug-96	Inj Between 16-1, 16-3	10	21800	0.762	8.85E-14
7-Aug-96	Inj Behind 18-1 (Open hole behind)	10	5800	4.1	1.05E-13
7-Aug-96	Inj Between 18-1, 18-4	1	16900	1.46	7.43E-15
8-Aug-96	Inj Between 18-1, 18-3	0.99	17400	0.762	1.12E-14
8-Aug-96	Inj Between 16-2, 16-4	0.5	18600	0.762	5.27E-15
8-Aug-96	Inj Behind 18-4	10	5800	1.46	2.30E-13
8-Aug-96	Inj Behind 18-4	10	5700	1.46	2.34E-13

Table 3. Comparison of air permeability before and after heating of the SHT block.

Location	Permeability (m ²) Pre Heating	Permeability (m ²) 25-Nov-96	Permeability (m ²) 4,5-Feb-97	Ratio Feb97/Preheat
Inj Behind 16-4	1.10E-14	2.58E-15	2.67E-15	0.24
Inj Behind 18-4	1.73E-13	7.93E-14	8.05E-14	0.46
Inj Between 16-2, 16-4	5.27E-15	2.83E-15	3.81E-15	0.7
Inj Between 16-1, 16-3	8.85E-14	9.03E-14	9.56E-14	1.1
Inj Between 18-1, 18-3	1.12E-14	1.08E-14	1.12E-14	1.0

Table 4. Calculated inflow rate of condensate into Borehole 16, Zone #3, based upon sample size collected and buildup of pressure in the zone.

Sample Collection Date	Sample Size	Calculated Infiltration Rate (Sample Volume /Time Elapsed)	Expected Value based upon ΔP (Horizontal Area of Wellbore × Head / Time Elapsed)
November 25, 1996	~5.5 liter	153 ml/day	149 ml/day
February 4, 1997	5.5 liter	78 ml/day	87 ml/day
February 27, 1997	1.52 liter	68 ml/day	92 ml/day

DRAFT DISCLAIMER

This contractor document was prepared for the U.S. Department of Energy (DOE), but has not undergone programmatic, policy, or publication review, and is provided for information only. The document provides preliminary information that may change based on new information or analysis, and is not intended for publication or wide distribution; it is a lower level contractor document that may or may not directly contribute to a published DOE report. Although this document has undergone technical reviews at the contractor organization, it has not undergone a DOE policy review. Therefore, the views and opinions of authors expressed do not necessarily state or reflect those of the DOE. However, in the interest of the rapid transfer of information, we are providing this document for your information.